Academic Journal of Science and Technology
ISSN: 2771-3032 | Vol. 15, No. 1, 2025

Analysis of Microscopic Mechanical Properties of Conglomerate Based on Nanoindentation Technology

Yangyang Zhou[1, *], Wen Wang[1]

[1] School of Energy Science and Engineering, Henan Polytechnic University, Jiaozuo 454003, China

* Corresponding author. E-mail address: zyy1050885023@163.com

Abstract: In order to reveal the microstructure control mechanism of the thick conglomerate layer in the process of rock burst inoculation and occurrence in Yima mining area, the mineral composition, cementation structure and micromechanical characteristics of typical conglomerate samples were systematically analyzed based on scanning electron microscope (SEM) and nanoindentation technology. The results show that the conglomerate in this area is densely cemented and the particles are closely arranged. The cements are mainly clay minerals, and some areas are associated with calcite and iron cements. The micro-fractures are developed along the particle boundary and the interface of the cement, showing a certain structural brittleness. The nanoindentation test reveals that there are obvious differences in mechanical properties of conglomerate in different micro-intervals, reflecting its heterogeneity and anisotropy characteristics at the micro-scale. The heterogeneity of microstructure and fracture development characteristics can easily lead to local stress concentration, which is one of the important microscopic factors inducing rock burst. The research results reveal the material basis and evolution mechanism of conglomerate rock burst disaster from a micro perspective, and provide theoretical support for the accurate identification and effective prevention and control of rock burst in extremely thick conglomerate strata in Yima mining area.

Keywords: Conglomerate; microstructure; scanning electron microscope; nanoindentation; rock burst; yima mining area.

1. Introduction

The Yima mining area is located in the middle of the Shanyu fault block on the southern margin of the North China platform. It is one of the important coal resource bases in the central and western regions of China. It has typical characteristics such as deep burial, thick coal seam and complex structure. In recent years, with the gradual advancement of resource exploitation to the deep, mine rock burst disasters have shown frequent, sudden and high-energy characteristics, which seriously threaten the safety of underground operations and the continuous production of mines. Especially in some areas, the huge thick conglomerate layer occurring in the roof or interlayer of the main coal seam has become an important geological background factor in the process of rockburst inoculation and release.

As a kind of composite rock composed of gravel, matrix and cement, the physical and mechanical properties of conglomerate are highly dependent on the microstructure characteristics, such as cementation type, particle arrangement, micro-fracture development and mineral composition distribution. Zhang et al.[1] used the nanoindentation test method to explore the microscopic mechanical properties of granite. The research results provide a new idea for deducing the macroscopic mechanical properties of rock from the microscale. Daniele et al.[2] conducted an in-depth analysis of the meso-mechanical properties of clay rock by means of nanoindentation experiments. Meng et al.[3] and Sun et al.[4] analyzed the mechanical properties and failure mechanism of coal at nanometer scale by means of nanoindentation test, which provided an important supplement for the in-depth study of the physical and mechanical properties of coal. Through the nanoindentation test, Lu et al.[5] discussed the micro-shear mechanical properties and failure modes of the grouting sandstone structural plane, revealed the mechanical variation law of the slurry-rock bonding interface and the transition zone, and provided a theoretical basis for optimizing the grouting reinforcement effect. Zhang et al.[6] evaluated the multi-scale mechanical properties of conglomerate based on nanoindentation test and homogenization method (Mori-Tanaka), and successfully realized the cross-scale prediction of mechanical properties of conglomerate. Ma et al.[7] are good methods to explain the variability of macroscopic rock elastic modulus. Ayatollahi et al.[8] studied the elastic modulus and hardness of several granites by nanoindentation technique. Zhu et al.[9] measured the mechanical properties of cement slurry and natural rock by this technique, and determined the Young 's modulus and hardness of each mineral phase by statistical analysis of a large number of experimental data. Combined with nanoindentation test and numerical calculation, Kim et al.[10] estimated the elastic modulus of rock and verified the consistency of the test and modeling methods. Sun et al.[11] studied the mechanical properties and creep properties of coal by nanoindentation. Yang et al.[12] and Liu et al.[13] evaluated the mechanical properties of shale, and analyzed the relationship between the mechanical indexes of shale. Si and Cla et al.[14][15] studied the mechanical properties and mineral composition of shale by nanoindentation technique.

Studies have shown that rocks with dense structure, high cementation strength and micro-cracks are prone to local instability under high ground stress and induce rock burst. However, at present, the research on the mechanical heterogeneity of conglomerate at the micro-scale and its effect on the disaster-causing effect of rock burst is still weak, especially in the context of complex structural areas and typical mining areas. The systematic analysis needs to be strengthened.

In view of this, this paper takes the typical thick

conglomerate layer in Yima mining area as the research object, and uses scanning electron microscope (SEM) and nanoindentation technology to comprehensively analyze the structural characteristics and mechanical response of conglomerate from the micro level, aiming to reveal the control mechanism of conglomerate microstructure on the evolution process of rock burst. The research results can provide theoretical basis and practical guidance for the cognition of disaster-causing law and prevention and control technology of rock burst under similar formation conditions in Yima mining area.

2. Petrological Characteristics of Conglomerates

X-ray diffraction (XRD) analysis and scanning electron microscope (SEM) observation of fine-, medium-, and coarse-grained conglomerate samples (Fig.1) revealed the mineral composition of the conglomerates and their microstructural characteristics.

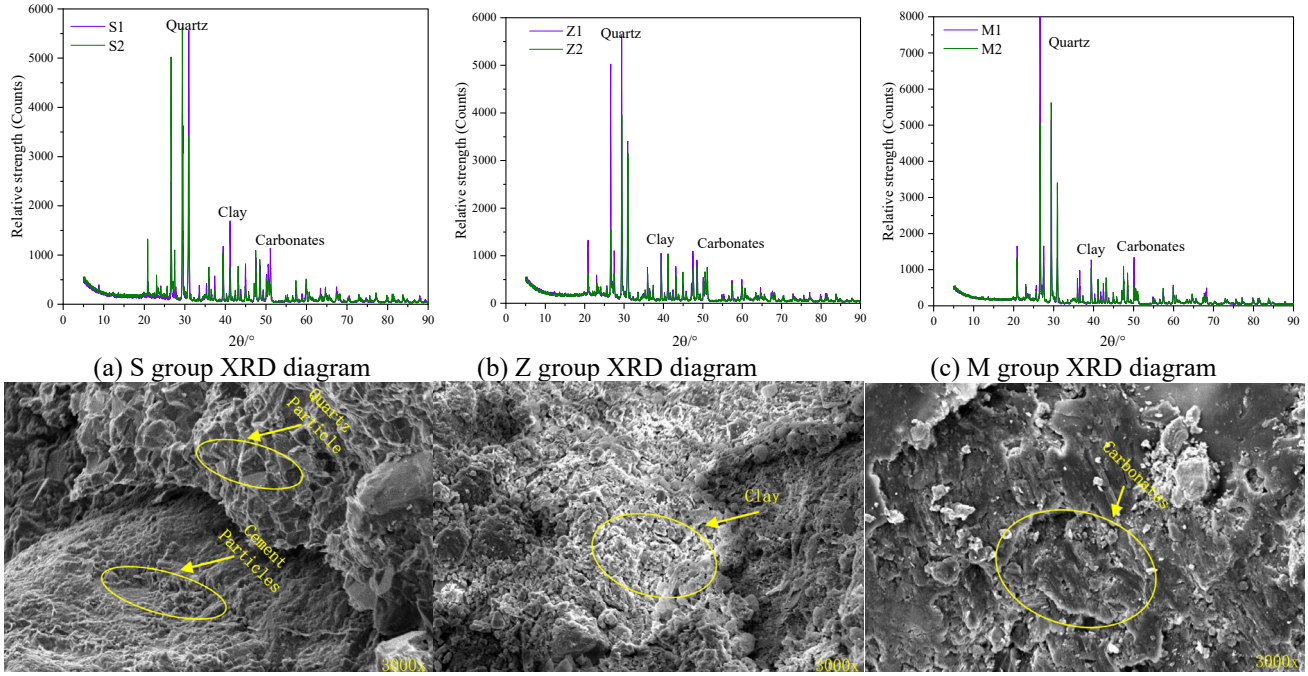

(a) S group XRD diagram (b) Z group XRD diagram (c) M group XRD diagram

(d) SEM diagram

Figure 1. Mineral composition and microstructure characteristics of conglomerate with the same particle size

XRD patterns (Fig.1 a-c) show that the main mineral components of the three types of conglomerates are quartz minerals (peak relative intensities of 6000, 5000, and 8000, respectively), carbonate minerals (peaks in the range of 3000-6000), and clay minerals (peaks in the range of 1000-4000). The relative intensity of quartz minerals in the fine- and coarse-grained conglomerates is significantly higher than that in the medium-grained conglomerates, suggesting that their content is significantly affected by grain-size sorting. Carbonate minerals have the highest proportion in the medium-grained conglomerates, which may be related to the hydrochemical conditions of their depositional environments. The content of clay minerals shows a decreasing trend in the three types of conglomerates, which is consistent with the change of pore structure caused by the increase of grain size.

SEM micrographs (Fig.1d) further validate the results of the XRD analysis and provide detailed information on the micromorphology of the minerals:

Quartz minerals (Fig.1d-M1 area) mostly show typical hexagonal or hexagonal-like crystal shapes, with flat crystal surfaces and sharp edges, and grain sizes ranging from 20-50 μm, and dissolution pits can be seen on the surfaces of some grains, suggesting that the diagenetic process was modified by fluid action.

The carbonate minerals (Fig.1d-M2 area) are mainly calcite, characterized by cubic or rhombic dodecahedron crystal morphology, with uniform grain sizes (about 10-30 μm) and regular cleavage surfaces between the crystals, reflecting its primary sedimentary genesis. The presence of dolomite microcrystals (grain size <5 μm) in local areas may be a product of late diagenesis.

Clay minerals (Fig.1d-S1, Z1 area) are mainly illite and montmorillonite, which are typical scale-like or plate-like aggregates, with the thickness of the lamellae less than 1 μm, and oriented along the pore edges. Micron-sized intergranular pores (pore diameters of 0.5-2 μm) are developed between the clay minerals, and some of the pores are filled by siliceous or ferruginous cement, suggesting modification of the pore structure by late cementation.

The coupled analysis of XRD and SEM results shows that the mineral composition of the conglomerates has a significant correlation with the microstructure: quartz minerals support the conglomerate skeleton as rigid particles, and their high content (especially in the coarse-grained conglomerates) enhances the compressive strength of the rocks; carbonate minerals fill intergranular pores through cementation, which lowers the permeability but improves structural densification; and the directional arrangement of clay minerals and the development of microporosity The directional arrangement of clay minerals and the development of microporous spaces may become an advantageous transportation channel for fluids, and their water absorption

and swelling characteristics pose potential risks to the long-term stability of the rocks. In addition, the quartz content in the giant conglomerate is more than 50% (Fig.1 a-c), and its high hardness and low toughness give the rock strong compressive strength. under the high stress environment in the depth, the rigid skeleton of quartz grains is easy to form a stress concentration zone, and the energy accumulation rate is far more than the dissipation capacity, which leads to sudden brittle rupture, releasing the elastic strain energy, and triggering the impact ground pressure. SEM observation shows the dissolution phenomenon (Fig.1 d-M1), which further weakens the intergranular bonding and exacerbates the risk of rupture.

3. Principles and Methods of Nanoindentation Experiments

3.1. Principle of nanoindentation experiment

The basic principle of nanoindentation is to press a tip indenter with known hardness, elastic modulus and other sample parameters into the tested sample with unknown parameters to obtain the load-displacement curve (P-h curve), and obtain the mechanical parameters of the tested sample through scientific analysis of the P-h curve. Figure 1 is a typical nanoindentation loading and unloading curve diagram. Where Pm is the maximum load, hl is the indentation depth when the maximum load is just reached, that is, the initial indentation depth of the holding platform segment, hm is the maximum indentation depth, h is the residual indentation depth after complete unloading, hc is the indentation contact depth, S is the slope at the top of the unloading curve. $S = dP / dh \,|\, h_m$, is the contact stiffness. Through these parameters, the elastic modulus and hardness of the sample can be obtained by using the Oliver-Pharr elastic parameter calculation method.

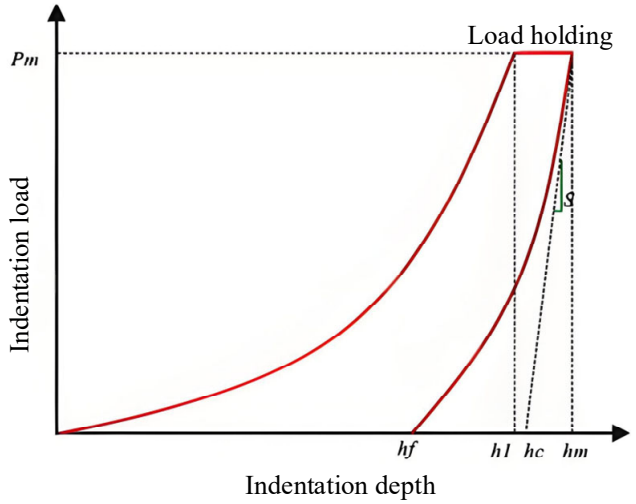

Figure 2. Relationship between indentation depth and load of nanoindentation

As shown in Fig.2, there is the following relationship between the contact stiffness and the reduction modulus Er of the sample :

$$E_r = \frac{\sqrt{\pi}}{2\beta\sqrt{A}} S \tag{1}$$

Among them : A is the contact area between the indenter and the tested sample ; for Berkovich indenter and Vickers indenter, β is 1.034 and 1.012, respectively. The relationship between the true elastic modulus E and the reduction modulus Er of the tested sample is as follows :

$$\frac{1}{E_r} = \frac{1-v_i^2}{E_i} + \frac{1-v^2}{E} \tag{2}$$

Where E and v are the elastic modulus and Poisson 's ratio of the tested sample, and Ei and vi are the elastic modulus and Poisson 's ratio of the indenter. The elastic modulus and Poisson 's ratio of the diamond indenter are 1141 GPa and 0.07, respectively. The indentation hardness can be calculated by the following formula :

$$H = \frac{P_{\max}}{A_c} \tag{3}$$

The contact area Ac is related to the indentation contact depth h_c : $A_c \approx \alpha h_c^2$, α is a parameter related to the shape of indenter. For Berkovich indenter, α = 24.5.

According to the classical linear elastic fracture mechanics theory, the energy release rate Gc in the critical state is defined as the energy dissipated per unit area of crack propagation :

$$G_c = \frac{W_c}{A_{fra}} \tag{4}$$

Wc is the fracture energy, and Afra is the area of the fracture energy release area, that is, the contact area Ac (h_m) at the maximum indentation depth. The critical stress intensity factor K_{IC}, i.e. fracture toughness, can be calculated by the following formula.

$$K_{IC} = \sqrt{G_c \frac{E}{1-v^2}} \tag{5}$$

Therefore, as long as the fracture energy Wc is characterized. The fracture toughness value can be obtained by energy method. For the nanoindentation test, due to the small size of the tip and edge of the indenter, even under the action of small external force, the stress singularity or concentration will inevitably occur in the area near the tip and edge of the indenter, which is greater than the strength of the sample. Therefore, for brittle or quasi-brittle specimens, regardless of the applied stress level, the specimen will inevitably fracture near the tip and edge of the indenter. At the same time, under the pressure, the whole sample under the pressure head projection surface undergoes different degrees of plastic deformation. In general, the plastic deformation and local fracture of the specimen occur simultaneously during the indentation test.

If the indentation measurement process is considered to be a static or quasi-static process, and the factors such as system error and heat dissipation are ignored, the relationship between the total energy W_T and the fracture energy W_C applied during the whole indentation process can be expressed as : According to the energy conservation relationship, the relationship between the total energy WT and the fracture energy W_C applied during the whole indentation experiment can be expressed as :

$$W_C = W_T - W_E - W_P \tag{6}$$

Among them, WE is the elastic energy of the sample during the measurement process, and WP is the pure plastic work. WT and WE can be directly obtained by the P-h curve of the indentation test, while WP needs to be calculated by the model.

In the following, the total energy coefficient Vt and the elastic energy coefficient Ve are used as the basic parameters of the energy model to characterize the energy parameters and fracture parameters, which are defined as the ratio of the calibrated loading energy to the total energy and the ratio of the calibrated unloading energy to the elastic energy.

$$V_t = \frac{W_1 + W_2}{W_2} \tag{7}$$

$$V_e = \frac{W_3 + W_4}{W_4} \tag{8}$$

Among them, W_2 and W_4 are the total energy dissipated during loading and the elastic energy recovered during unloading, respectively. W1 + W2 is the calibration loading energy, that is, the calibration energy that may be dissipated when the indenter with a specific geometric shape is pressed into any sample ; similarly, $W_3 + W_4 + W_5$ is the calibration unloading energy. The graph area corresponding to each energy is shown in Fig. 3. The Vt and Ve values are not only related to energy, but also characterize the loading and unloading curves. A large number of studies have shown that the loading and unloading sections of the test curve should meet the exponential function relationship.

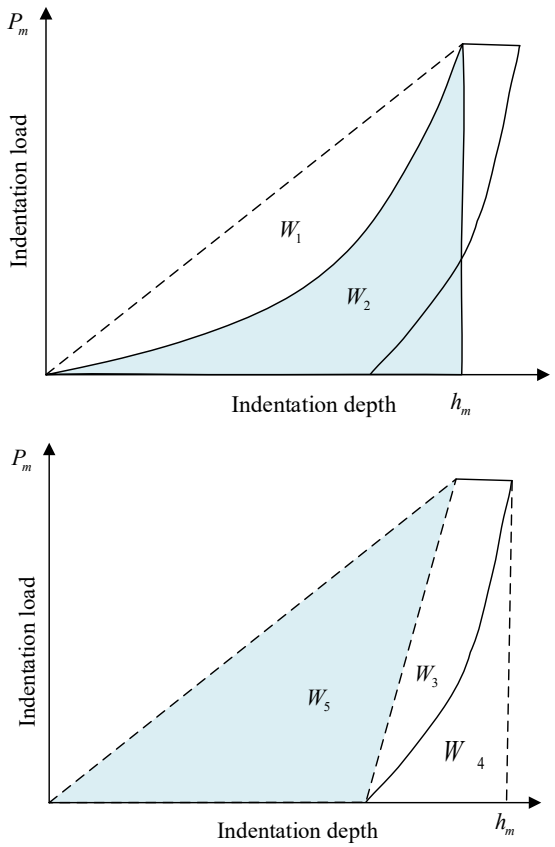

Figure 3. The energy division diagram of the test loading-unloading curve

$$P = \begin{cases} K_m h_m = P_m \left(\dfrac{h}{h_1}\right)^{2V_t - 1}, & 0 \le h < h_1 \\ P_m, & h_1 \le h \le h_m \\ K_1(h - h_f) = P_m \left(\dfrac{h - h_f}{h_m - h_f}\right)^{2V_e - 1}, & h_m > h > h_f \end{cases} \tag{9}$$

For the elastic-plastic indentation test process that satisfies the above formula, the total energy can be expressed as:

$$W_T = \frac{P_m h_1}{2V_t} + P_m(h_m - h_1) \tag{10}$$

The elastic energy We of the unloading process can be expressed as :

$$W_E = W_4 = \int_{h_f}^{h_m} P_m \left(\frac{h - h_f}{h_m - h_f}\right)^{2V_e - 1} dh = \frac{P_m}{2V_c}(h_m - h_f) \tag{11}$$

For pure elastic-plastic specimens, there is the following relationship between W_T and W_P :

$$\frac{W_P}{W_T} = \frac{W_T - W_E}{W_T} = \frac{1 + \dfrac{1}{2V_t} \cdot \dfrac{h_1}{h_m} \cdot \dfrac{1}{2V_e} 1 - \dfrac{h_f}{h_m}}{1 + \dfrac{1}{2V_t} \cdot \dfrac{h_T}{h_m}} \tag{12}$$

For non-pure elastic-plastic samples, the fracture of the sample during the nanoindentation test will also consume some energy, but the formula (13) still holds. Therefore, through formula (6) ~ formula (12), the fracture energy WC can be obtained, and then the fracture toughness of the sample can be obtained. The specific parameter calculation results are shown in table 1.

Table 1. Calculation results of nanoindentation parameters

	$W_c \times 10^6$	$A_c \times 10^6$	K_{IC}	V_t	V_e	B	T
S_Gravel	5.43	21.86	1.55	1.35	1.96	0.36	0.65
S_Gravel-matrix	3.72	233.90	0.42	3.79	2.24	0.22	1.59
S_ Matrix	32.24	1024.93	0.28	1.35	2.54	0.07	7.66
Z_Gravel	2.92	21.55	2.02	1.29	1.80	0.88	1.05
Z_Gravel-matrix	5.99	43.13	1.42	1.18	1.90	0.47	8.18
Z_ Matrix	0.88	135.96	0.45	1.47	1.53	0.28	8.44
M_Gravel	0.77	3.95	3.31	1.53	3.35	0.98	1.69
M_Gravel-matrix	1.10	12.89	2.24	2.23	3.89	0.83	4.03
M_ Matrix	2.65	350.48	0.34	4.57	6.39	0.43	20.31

3.2. Characteristics of displacement-load relationship of conglomerate loading and unloading

The process of conglomerate nanoindentation experiment includes four stages :

1)surface approaching stage : using the continuous stiffness measurement method, the 10nm/s descending speed makes the needle slowly close to the surface of the sample. When the contact stiffness increases suddenly, it indicates that the needle has touched the surface of the sample ;

2) Loading stage : load control loading mode is adopted. The indenter is vertically pressed into the specified position of the sample at a loading rate of 5000μN/s until the maximum load 5000μN is predetermined. At this time, indentation damage is formed inside the sample.

3) Load holding stage : when the indentation load reaches the maximum load, the load is maintained for 2s. It can be seen from Fig. 3 that the corresponding displacements of different indentation points of conglomerate are different, which is speculated to be related to the difference of creep degree of conglomerate in different sedimentary facies.

4) Unloading stage : At the unloading rate of 100μN / s, the indenter was kept away from the sample surface until completely unloaded.

In the loading stage, with the increase of the downward displacement of the indenter, the load also increases; when the maximum intrusion depth is reached, the indenter begins to unload, its upward displacement gradually decreases, and the load decreases simultaneously. As can be seen from Fig. 4, at the same location of the indentation point, the overall indentation depth corresponding to the maximum load of fine-grained conglomerate (S group, the particle size range is 2-25 mm), medium-grained conglomerate (Z group, the particle size range is 2-45 mm) and coarse-grained conglomerate (M group, the particle size range is 2-60 mm) samples shows a decreasing trend. This shows that under the action of external load, the internal damage of the 3 conglomerate is gradually intensified, and the absorption efficiency of the external energy of the fine-grained conglomerate is relatively high in the process of pressure head intrusion. This is because the fine grained conglomerate particles are closely arranged, the matrix content is high, easy to produce uniform plastic deformation, which shows a higher absorption efficiency of external energy; coarse grained conglomerate due to the larger particle size, less matrix content, under load mainly for brittle failure, energy absorption efficiency is low. Within the same group of specimens, there are significant differences in the depth of penetration at different points of penetration: the smallest depth of penetration at the gravel, followed by the gravel-matrix junction, and the largest depth of penetration at the matrix position. Gravel particles usually have higher hardness and strength, so they show stronger load resistance and lower deformation ability, resulting in a smaller penetration depth; the matrix is generally cementitious or fine-grained particles with lower hardness and strength, and stronger plastic deformation ability, so it is easier to be compressed, showing a greater penetration depth. There may be stress concentration effect and micro fracture propagation at the interface, which leads to the mechanical properties between gravel and matrix. These regular characteristics can indirectly reflect the brittleness and mechanical properties of different conglomerates, and further reveal the microscopic failure mechanism of conglomerates with different particle sizes.

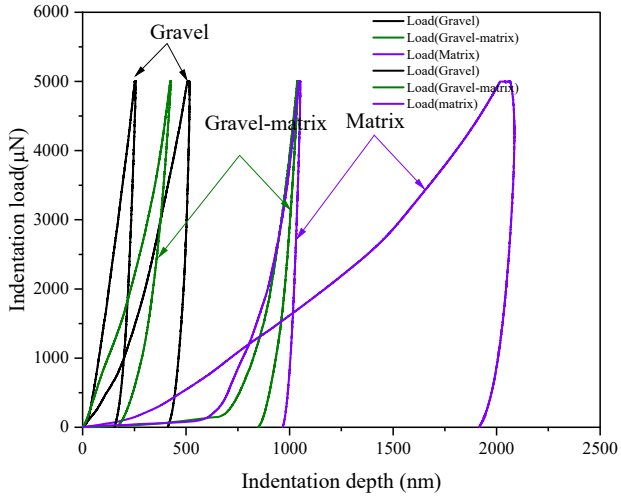

(a) fine-grained conglomerate (S group)

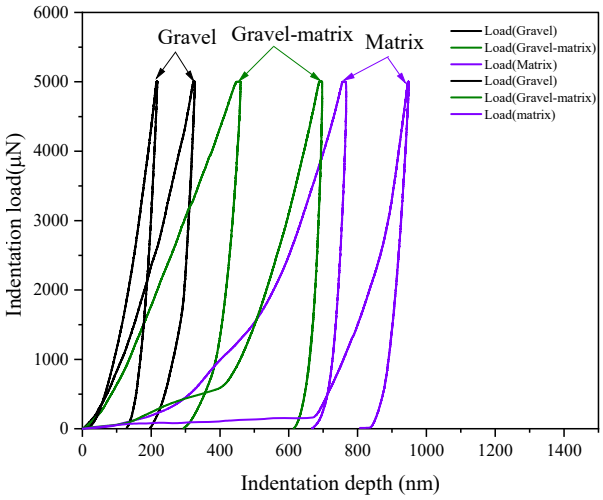

(b) Medium-grained conglomerate (Z group)

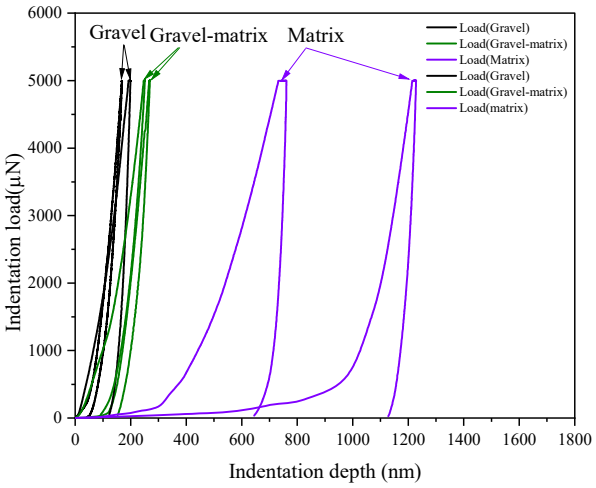

(c) Coarse-grained conglomerate (M group)

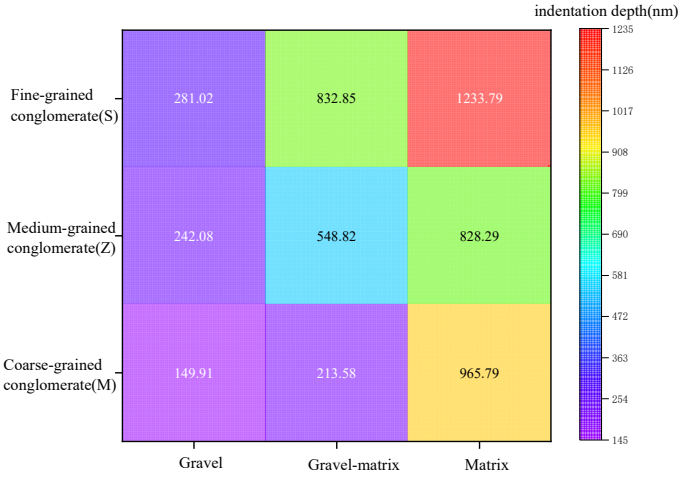

(d) Thermal diagram of average indentation depth of conglomerate

Figure 4. Displacement-load curve and thermal diagram of conglomerate nanoindentation loading

3.3. Elastic modulus and hardness characteristics of conglomerate

The buried depth of Yima mining area is large, the level of ground stress is high, and the stiffness of conglomerate is large, which leads to the accumulation of elastic deformation. The difference in hardness and elastic modulus between gravel and matrix leads to prominent stress transfer and concentration effect, which is easy to cause sudden release of stress. The elastic modulus and hardness obtained by nanoindentation test can provide important theoretical and practical basis for the prediction, prevention and control and safety design of rock burst. These parameters can not only reflect the microscopic damage evolution process of rock, but also guide the implementation of stress distribution analysis, support optimization and stress release measures, which lays a foundation for improving the mining safety and anti-impact ability of mining area. According to the calculation method of formula (1) ~ formula (3), the elastic modulus / hardness of fine-grained conglomerate (S group), medium-grained conglomerate (Z group) and coarse-grained conglomerate (M group) is obtained as Fig.5. The hardness and elastic modulus of coarse-grained conglomerate (M group) are significantly higher than those of the other two groups, reflecting that coarse-grained conglomerate (M group) has high hardness and high elastic modulus, showing strong rigidity, high deformation resistance, significant brittleness and high energy storage characteristics, which is easy to form stress concentration and sudden fracture.

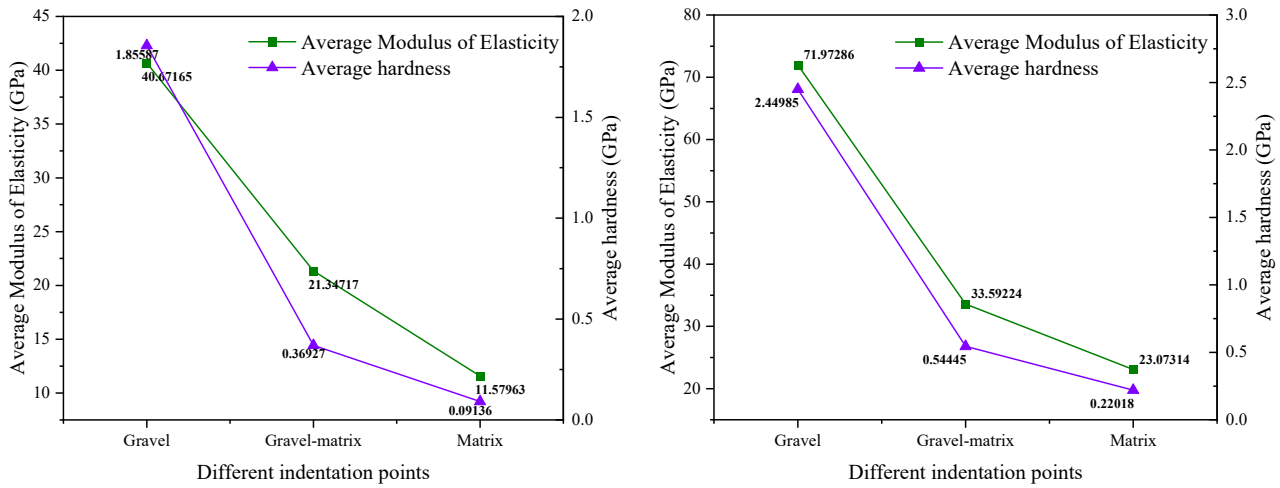

(a) fine-grained conglomerate (S group) (b) Medium-grained conglomerate (Z group)

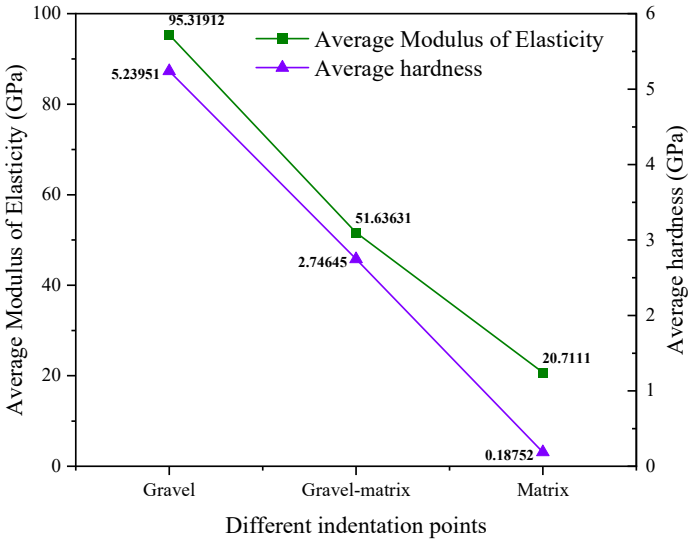

(c) Coarse-grained conglomerate (M group)

Figure 5. Characteristics of elastic modulus and hardness of conglomerate

Fig.5 shows the differences in elastic modulus and indentation hardness of gravel, gravel-matrix and matrix at different indentation points. In the same group, the gravel showed the highest elastic modulus and indentation hardness at each indentation point, followed by the gravel-matrix, while the matrix had the lowest elastic modulus and hardness. Gravel is usually composed of hard minerals, with large particles, high density and strong structural rigidity, which makes it show high deformation resistance under compression, and thus has high elastic modulus and hardness. In contrast, the elastic modulus and hardness of the gravel-matrix are lower, because the existence of the matrix weakens the overall mechanical properties. The matrix is generally composed of soft minerals (such as clay or rock debris), with low density and weak compressive strength, resulting in low elastic modulus and hardness, which is prone to deformation and compression, thus affecting the mechanical performance of the whole sample. In general, the high elastic modulus and hardness of the gravel are mainly derived from its hard mineral composition and larger particle size, while the low elastic modulus and hardness of the matrix are derived from its soft mineral composition and smaller particle size. In addition, under the same indentation point, gravel samples with different particle sizes show different mechanical properties. The sample with coarse particle size has the highest elastic modulus and hardness, followed by the medium particle size, and the fine particle size has the lowest elastic modulus and hardness. The larger particle size and higher structural rigidity of the coarse-grained sample enable it to resist deformation and withstand external forces more effectively, thus showing higher elastic modulus and hardness. On the contrary, the fine-grained sample is prone to deformation due to its small particle size, low density, large contact area and small friction force, so its elastic modulus and hardness are low.

3.4. Fracture toughness characteristics of conglomerate

Fracture toughness of fine grained conglomerate (Group S), medium grained conglomerate (Group Z) and coarse grained conglomerate (Group M) calculated according to Equations (4)~(12). Fig.6 shows fracture toughness differences of gravel, gravel matrix and matrix at different injection points. Within the same group, fracture toughness of gravel is the highest, followed by gravel matrix and matrix is the lowest. Gravel is usually composed of hard minerals, larger particles and higher density, which makes it show strong fracture resistance under external forces. Larger particles and higher density improve gravel's ability to resist external impact and crack propagation, thus showing higher fracture toughness. Hard

mineral composition also limits crack propagation at the interface between particles, increasing crack resistance. In contrast, although the gravel-matrix is supported by the crack resistance of the gravel particles, the soft components in the matrix reduce the overall toughness. The matrix is generally composed of softer minerals, and its lower strength and compressive resistance make cracks easier to propagate inside the matrix, thereby reducing fracture toughness. The matrix has the lowest fracture toughness because its particles are small and lack strong structural support, and cracks propagate easily. The fracture toughness of coarse grain samples is the highest, followed by medium grain samples, and the fracture toughness of fine grain samples is the lowest. The larger grain size and higher density of coarse grain samples make their structure stronger and stiffer. Coarse grained gravel is more difficult to deform or crack propagate under external force, so it exhibits higher fracture toughness. Contact points between large grained gravel increase friction and compressive strength, thus further improving fracture toughness. Fracture toughness of medium grained gravel is between coarse grained gravel and fine grained gravel. Deformation resistance and crack resistance are slightly lower than coarse grained gravel due to smaller grained gravel, but close contact between grains still endows certain crack resistance and toughness. Fine-grained samples have smaller particles, fewer contact points and lower friction force, resulting in poor deformation resistance and crack propagation resistance.

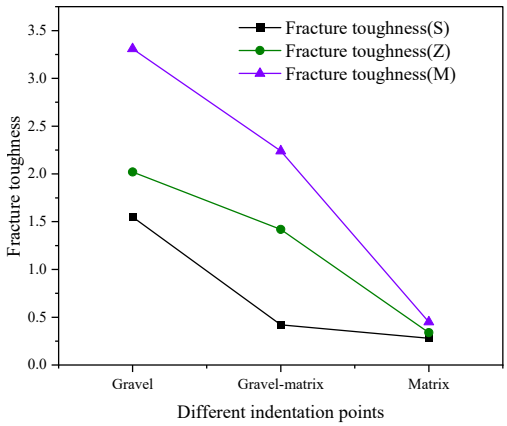

(a)Fracture Toughness Characteristics at Different Indentation Points

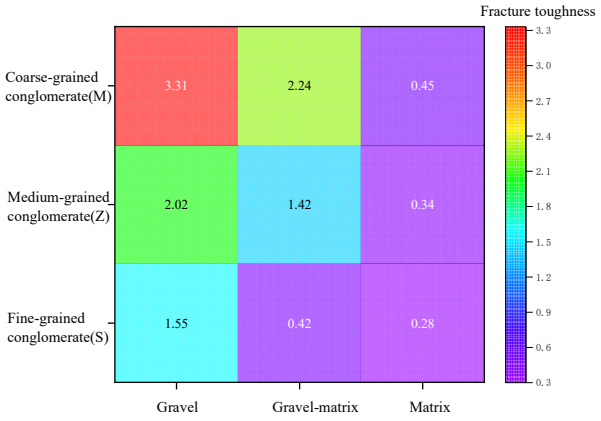

(b) Thermal diagram of fracture toughness

Figure 6. Characteristics of fracture toughness of conglomerate

As shown in Fig.7, fracture toughness has a linear positive correlation with elastic modulus and hardness, and a linear negative correlation with indentation depth, with correlation coefficients above 0.85. High elastic modulus and hardness make it difficult for the specimen to undergo local plastic deformation when subjected to external force, thus making it more difficult for cracks to propagate. The specimen can still maintain high stability and integrity under the action of higher external force. Therefore, the higher the elastic modulus and hardness, the higher the fracture toughness, the higher the fracture resistance and deformation resistance of the specimen, and the negative correlation between the indentation depth and fracture toughness also indicates the influence of crack propagation and plastic deformation on the fracture process.

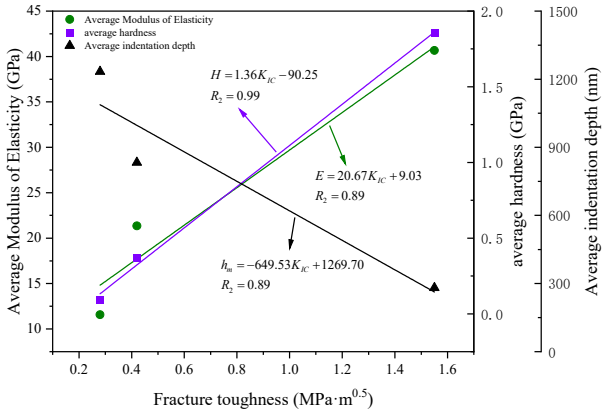

(a) fine-grained conglomerate (S group)

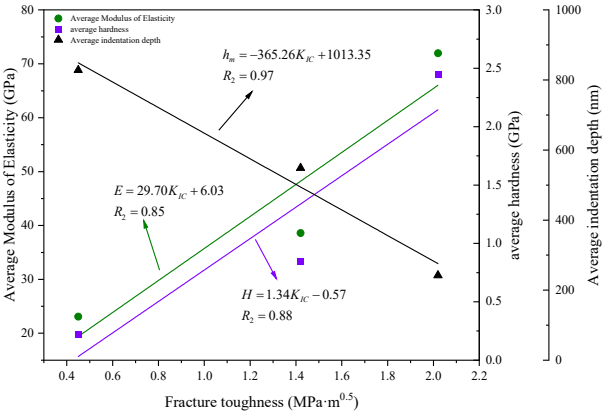

(b) Medium-grained conglomerate (Z group)

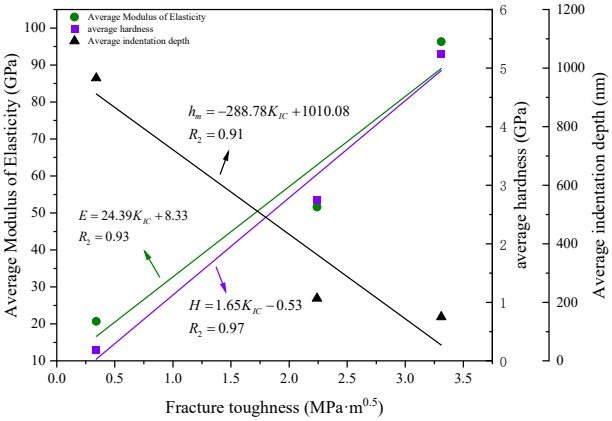

(c) Coarse-grained conglomerate (M group)

Figure 7. The relationship between fracture toughness, elastic modulus and hardness of conglomerate

4. Conclusion

(1) The fracture toughness of the conglomerate is positively correlated with the elastic modulus and hardness, and negatively correlated with the indentation depth. The indentation depth of matrix is 4.49 times that of gravel, 1.89 times that of gravel-matrix, and 2.37 times that of gravel. The high elastic modulus and hardness make the conglomerate have high crack resistance and stability, but the larger indentation depth will aggravate the plastic deformation and crack propagation, and reduce the fracture toughness.

(2) Conglomerates with different particle sizes show significant mechanical differences. Coarse-grained conglomerate has high hardness, elastic modulus and brittleness coefficient, showing hard brittleness and elastic response characteristics. The medium-grained conglomerate is between hard brittleness and plasticity, and has certain toughness and crack resistance. The fine-grained conglomerate shows plastic characteristics, with the lowest hardness and elastic modulus and strong energy absorption capacity.

Acknowledgements

The authors gratefully acknowledge the financial support from Henan University Science and Technology Innovation Talent Plan Project (23HASTIT011).

References

[1] Zhang Fan, Guo Hanqun, Zhao Jianjian et al.. Experimental study on micromechanical properties of granite [J].Journal of Sample Mechanics and Engineering, 2017,36 (S2) : 3864-72.

[2] BARTIER D, AUVRAY C. Determination of elastic modulus of claystone: Nano-/micro-indentation and meso-compression tests used to investigate impact of alkaline fluid propagation over 18 years [J]. Journal of Rock Mechanics and Geotechnical Engineering, 2017, 9(03): 133-40.

[3] Meng, Niu, Xia et al.. Study on mechanical properties and failure mechanism of coal at nanoscale [J]. Journal of Sample Mechanics and Engineering, 2020,39 (01) : 84-92.

[4] Sun Changlun, Li Guichen, ELGHARIB G M, et al. Experimental study on mechanical properties of crushed coal samples based on nanoindentation technology [J]. Coal Journal, 2020,45 (S2) : 682-91.

[5] Lu Yinlong, He Mengqi, Li Wenshuai, et al. Micromechanical Mechanism of Grouting Reinforcement on Specimen Structural Plane and Structural Optimization of Slurry-Rock Bond Interface [J]. Journal of Specimen Mechanics and Engineering, 2020, 39(09): 1808-18.

[6] Zhang Zhaopeng, Zhang Shicheng, Shi Shanzhi, et al. Evaluation of Multi-scale Mechanical Properties of Conglomerate Based on Nanoindentation Experiment and Homogenization Method-Taking Tight Conglomerate Reservoir in South Slope of Mahu Sag as an Example [J]. Journal of Specimen Mechanics and Engineering, 2022, 41(05): 926-40.

[7] MA Z, PATHEGAMA GAMAGE R, ZHANG C. Application of nanoindentation technology in rocks: a review [J]. Geomechanics and Geophysics for Geo-Energy and Geo-Resources, 2020, 6: 1-27.

[8] M.R. A, ZARE N M, R. K S S, et al. Mechanical Characterization of Heterogeneous Polycrystalline Rocks Using Nanoindentation Method in Combination with Generalized Means Method [J]. JOURNAL OF MECHANICS, 2020, 36(6): 813-23.

[9] ZHU W, HUGHES J J, BICANIC N, et al. Nanoindentation mapping of mechanical properties of cement paste and natural rocks [J]. Materials Characterization, 2007, 58(11/12): 1189-98.

[10] HOKIBAN, PRAVATKARKI, YONG-RAKKIM. Nanoindentation Test Integrated with Numerical Simulation to Characterize Mechanical Properties of Rock Materials [J]. JOURNAL OF TESTING AND EVALUATION, 2014, 42(3): 787-96.

[11] SUN C, LI G, GOMAH M E, et al. Creep characteristics of coal and rock investigated by nanoindentation [J]. International Journal of Mining Science and Technology, 2020, 30(6): 769-76.

[12] YANG Z, WANG L, CHEN Z, et al. Micromechanical Characterization of Fluid/Shale Interactions by Means of Nanoindentation [J]. SPE RESERVOIR EVALUATION & ENGINEERING, 2018, 21(2): 405-17.

[13] LIU K, OSTADHASSAN M, BUBACH B. Applications of nano-indentation methods to estimate nanoscale mechanical properties of shale reservoir rocks [J]. Journal of Natural Gas Science and Engineering, 2016, 35: 1310-9.

[14] CAŁA M, CYRAN K, KAWA M, et al. Identification of Microstructural Properties of Shale by Combined Use of X-Ray Micro-CT and Nanoindentation Tests [J]. Procedia Engineering, 2017, 191: 735-43.

[15] SHI X, HE Z, LONG S, et al. Loading rate effect on the mechanical behavior of brittle longmaxi shale in nanoindentation [J]. INTERNATIONAL JOURNAL OF HYDROGEN ENERGY, 2019, 44(13): 6481-90.